



Research paper

Fuzzy conceptual spaces for dental shade analysis: A perceptually grounded approach with an open-source python framework

Rafael Vázquez-Conejo ^a,* Maria Tejada-Casado ^a, Luis Javier Herrera ^b, Razvan Ghinea ^a, Jose Manuel Soto-Hidalgo ^b

^a Department of Optics, University of Granada, Spain

^b Department of Computer Engineering, Automation and Robotics, University of Granada, Spain

ARTICLE INFO

Keywords:

Fuzzy conceptual spaces
Artificial intelligence
Dental shade analysis
Perceptual color modeling
Shade matching

ABSTRACT

Accurate tooth shade matching remains a challenging task in restorative dentistry due to the subjective nature of color perception and the limitations of visual and instrumental methods. This study presents a perceptually grounded and extensible artificial intelligence framework for dental shade analysis based on fuzzy conceptual spaces, implemented in the open-source Python library PyFCS (Python Fuzzy Color Spaces). The proposed methodology supports the construction of fuzzy color categories from dental shade guides and enables pixel-wise chromatic mapping and region-wise analysis of segmented dental samples. The framework was instantiated with the 16 shades of the VITA Classical Shade Guide. An initial controlled evaluation was conducted with twelve dental experts using an interface integrated into PyFCS. Expert-based annotations were collected for tooth regions and compared with system outputs using the full fuzzy Jaccard similarity metric, complemented by a secondary partial-overlap analysis. The highest agreement was observed in the middle third of the tooth, with a full fuzzy Jaccard similarity of 0.68 ± 0.30 and a partial-overlap Jaccard similarity of 0.76 ± 0.20 , whereas lower agreement and higher complete-disagreement rates were found in the cervical and incisal regions. These findings suggest that fuzzy conceptual spaces can provide an interpretable representation of perceptual ambiguity and gradual transitions between dental shades under controlled conditions. By supporting adaptation to different dental shade guides and institutional protocols, this contribution provides a flexible basis for the development of expert-informed, perceptually grounded tools for dental color analysis and future clinically oriented shade selection research.

1. Introduction

Color perception plays a central role in how humans interpret and communicate visual information (Palmer, 1999; Itten, 1974). Accurate modeling of this process is essential in a wide range of applications in computer vision and image processing (Kim et al., 2023; Rigueira et al., 2022), including tasks such as instance segmentation (Doe et al., 2022) and image harmonization (L. Li et al., 2025). Moreover, color-based reasoning has gained increasing relevance in industrial domains such as textiles, automotive coatings, and clinical dentistry (Cherfi et al., 2002; Li, 2024; Rashid et al., 2023a; Carrillo-Perez et al., 2022). In the dental field in particular, shade selection is a critical step in restorative and prosthetic procedures, requiring fine-grained chromatic accuracy to ensure natural-looking results. Traditionally, this task has relied on visual assessment using standardized clinical shade guides. However, extensive comparative studies have demonstrated that visual

shade selection methods sometimes suffer from limited accuracy and low reproducibility, with reported color differences (ΔE) ranging from 2.74 to 14.60 and matching rates as low as 22.5% (Rashid et al., 2023b; Gehrke et al., 2009a; Judeh and Al-Wahadni, 2009). These outcomes are strongly influenced by operator experience and environmental conditions (Jaffer and Al-kholani, 2024; Şahin and Ural, 2024).

In contrast, instrumental shade matching technologies, including spectrophotometers, colorimeters, digital photography, and smartphone-based tools, have shown improved performance, often producing ΔE values within clinically acceptable thresholds and achieving reproducibility rates above 90% when properly calibrated and used under controlled conditions (Kutkut et al., 2024; Tabatabaian et al., 2021; Morsy and Holiel, 2023). Nonetheless, these instrumental methods also have limitations: they require interpretation of numerical outputs, can

* Corresponding author.

E-mail addresses: rafaconejo@ugr.es (R. Vázquez-Conejo), mariatejadac@ugr.es (M. Tejada-Casado), jherrera@ugr.es (L.J. Herrera), rghinea@ugr.es (R. Ghinea), jmsoto@ugr.es (J.M. Soto-Hidalgo).

<https://doi.org/10.1016/j.engappai.2026.115437>

Received 12 June 2025; Received in revised form 9 June 2026; Accepted 11 June 2026

Available online 18 June 2026

0952-1976/© 2026 The Authors. Published by Elsevier Ltd. This is an open access article under the CC BY-NC-ND license (<http://creativecommons.org/licenses/by-nc-nd/4.0/>).

vary in effectiveness depending on the device, and may struggle to adapt flexibly to individual patient characteristics (Hardan et al., 2022). Compounding these technological challenges is the inherently subjective nature of color perception, which is shaped by cognitive, cultural, and environmental factors (Rosch, 1975, 1978). As a result, there is a persistent discrepancy between how color is digitally encoded and how humans perceive it, a phenomenon commonly referred to as the 'semantic gap' (Smeulders et al., 2000). Bridging this gap is especially critical in dentistry, where even subtle chromatic mismatches can significantly affect clinical outcomes and patient satisfaction. Despite the progress of digital shade matching technologies, important challenges remain in dental color assessment, particularly due to the subjective nature of color perception and the gradual transitions between neighboring shades. To address these limitations, this study introduces a framework based on fuzzy conceptual spaces, enabling the modeling of perceptual ambiguity and gradual color transitions in a clinically interpretable manner.

Fuzzy logic provides a powerful theoretical and practical framework to reduce this semantic gap (Berlin and Kay, 1991). By modeling color categories as fuzzy subsets in a perceptual color space, fuzzy systems capture the graduality and ambiguity inherent in human color interpretation (Rosch, 1978). However, most traditional fuzzy color modeling approaches rely on tedious perceptual experiments to define membership functions (Benavente et al., 2008; Menegaz et al., 2007), limiting their scalability and practical adoption. An alternative paradigm grounded in cognitive science is the theory of conceptual spaces (Gärdenfors, 2000, 2014), which offers a geometric representation for concepts in a multidimensional perceptual space. This theory is particularly effective in modeling categories like colors, where perceptual similarity plays a fundamental role. Building on this foundation, a formal approach to model fuzzy color categories within conceptual spaces was proposed (Chamorro-Martínez et al., 2016), enabling the representation of gradual transitions and overlapping regions between perceptual categories. This proposal constitutes the theoretical basis for the PyFCS library (Conejo et al., 2024), which operationalizes these concepts into a flexible and extensible software framework for constructing and analyzing fuzzy color spaces without the need for exhaustive experiments.

In this context, the contribution of the present work lies in adapting and extending the existing PyFCS framework for dental shade analysis, rather than in proposing a new fuzzy conceptual space algorithm. This paper proposes a practical approach based on PyFCS to learn and visualize a fuzzy color space aligned with the 16 shades (A1–A4, B1–B4, C1–C4, and D2–D4) of the VITA Classical Shade Guide — a standard widely used in dentistry (Fig. 1). Thanks to the extensible and modular architecture of PyFCS, we have integrated new functionalities into its graphical user interface to facilitate this process. In particular, we highlight the ease of use provided by this methodology, which allows users to model the full dental shade spectrum using fuzzy concepts without requiring manual calibration or psychophysical testing. The resulting fuzzy color space offers an intuitive 3D visualization of the gradual transitions between chromatic categories (shades) from VITA Classical Guide, capturing perceptual nuances that traditional Euclidean metrics in spaces like CIELAB often fail to distinguish.

Beyond the construction of fuzzy color spaces, this work introduces two complementary modules for pixel-level chromatic analysis and expert-based evaluation. First, a chromatic mapping system is developed to visualize fuzzy membership distributions across tooth images. This includes both grayscale mappings — representing the degree of membership to a specific fuzzy color — and full-color mappings based on the maximum membership principle. These visualizations support perceptual analysis of color distribution and are particularly valuable when working with highly similar shades, such as those in the VITA Classical Guide. Second, a clinical region segmentation module partitions each image into a 3×3 grid, corresponding to incisal, middle, and cervical thirds across left, central, and right columns.

For each of the nine regions, aggregated fuzzy possibility distributions can be computed using two strategies: maximum membership and normalized average. These summaries provide a region-wise chromatic interpretation aligned with dental diagnostic workflows. To support the controlled expert-based evaluation, a dedicated evaluation module was integrated into PyFCS, allowing experts to annotate shades and associated membership degrees across predefined regions. Expert annotations were compared to system outputs using the full fuzzy Jaccard similarity metric, complemented by a secondary partial-overlap analysis, providing an initial controlled assessment of expert alignment and interpretability.

The paper is organized as follows. Section 2 reviews the state of the art in dental shade matching, covering both visual and digital approaches, along with their reported limitations. Section 3 introduces the theoretical foundations of fuzzy color modeling based on conceptual spaces and provides a detailed characterization of the VITA Classical Shade Guide. Section 4 presents the design and implementation of the fuzzy shade matching framework, including the construction of the fuzzy color space, spatial mapping of chromatic regions, and the expert evaluation interface developed within PyFCS. Section 5 details the expert evaluation protocol, including participant selection, annotation methodology, and the fuzzy similarity metric used to assess system performance. Section 6 reports and discusses the experimental results, highlighting the agreement patterns between the anatomical regions of the teeth. Finally, Section 8 concludes the paper and outlines directions for future research.

2. Related work

Tooth shade selection is a key step in restorative dentistry, directly impacting both aesthetic and functional outcomes. Historically, visual methods based on standardized shade guides — such as the VITA Classical or VITA-3D-Master — have been the most widely used tools in clinical practice. However, these methods are highly subjective and depend heavily on clinician expertise, lighting conditions and individual visual sensitivity (Tabatabaian et al., 2021). Additionally, shade guides have been reported to have a relatively high coverage error of the dental chromatic space (ΔE ranging from 2.5 to over 4.8) (Ruiz-López et al., 2022). Therefore, numerous studies have reported considerable inconsistencies in shade selection outcomes using visual assessment alone. For example, other authors (Gehrke et al., 2009b) found match rates as low as 22.5% and color differences (ΔE) exceeding clinically acceptable thresholds in a significant number of cases. Other studies have echoed these findings, showing poor inter- and intra-operator reproducibility under real-world conditions (Rashid et al., 2023b; Judeh and Al-Wahadni, 2009).

In response to these limitations, a variety of instrumental shade-matching systems have been introduced, including spectrophotometers, colorimeters, intraoral scanners, digital photography, and smartphone-based solutions. When used under controlled conditions, these devices typically yield improved accuracy and reproducibility. Spectrophotometers, for instance, have been shown to achieve color difference values in the range of 0.09–3.2 and reproducibility rates exceeding 90% in laboratory settings (Kutkut et al., 2024; Morsy and Holiel, 2023). Some colorimeters have achieved reliability rates up to 99.6% (Kutkut et al., 2024), while digital cameras and smartphones have reported ΔE values generally within clinically acceptable ranges (Jorquera et al., 2022; Şahin and Ural, 2024). Nevertheless, the performance of these technologies is highly dependent on device calibration, ambient lighting, and the ability of clinicians to interpret numerical or visual outputs accurately. In fact, some studies suggest that experienced clinicians using visual methods can outperform instrumental systems under certain conditions (Jaffer and Al-kholani, 2024), further highlighting the complexity of the problem.

Recent advances in artificial intelligence have further expanded the use of color-based and image-based analysis in healthcare and



Fig. 1. The VITA Classical Shade Guide (VITA Zahnfabrik, 2025). The guide consists of 16 standardized shades grouped into four chromatic families (A–D) commonly used in clinical dental shade matching.

industrial inspection, including colorimetric sensing, wearable diagnostic platforms, wound assessment, and medical image analysis (Parakh et al., 2025; Wang et al., 2024; Chairat et al., 2023; Alnaggar et al., 2024; Salvi et al., 2026). These studies confirm the growing relevance of data-driven and intelligent methods for supporting color-dependent decision-making in complex environments. However, most existing approaches are primarily oriented toward prediction, detection, or classification accuracy, and typically provide crisp outputs that do not explicitly model the gradual transitions, overlap, and perceptual uncertainty that characterize human color interpretation. This limitation is especially relevant in dental shade matching, where clinically meaningful decisions often depend on subtle chromatic differences and ambiguous intermediate cases. In this context, the proposed fuzzy conceptual space framework complements current artificial intelligence approaches by providing a perceptually grounded and interpretable representation of dental color categories, allowing shade assignments to be expressed as fuzzy possibility distributions rather than as single-label decisions.

Despite these technological advancements, most digital systems still fail to bridge the “semantic gap” between objective color measurements and the way humans perceive color categories (Smeulders et al., 2000). Color difference formulas like CIELAB and CIEDE2000, although widely used, rely on Euclidean or perceptual distance metrics that assume crisp boundaries and uniform perceptual distribution—assumptions that do not hold in practical or clinical scenarios. Consequently, they are unable to capture the gradual transitions, overlaps, and ambiguities that characterize real human color experience, particularly in applications such as dental shade matching. This shortfall has prompted the exploration of fuzzy logic-based models that represent color categories as soft regions with graded membership, offering a more cognitively plausible and perceptually aligned alternative.

In the last decade, two main computational paradigms have emerged to address this challenge. The first relies on parametric fuzzy set models, using techniques such as Delaunay triangulation, fuzzy C-means clustering, and linear interpolation over color spaces like CIELAB or ISCC-NBS (Benavente et al., 2008; Menegaz et al., 2007; Herrera et al., 2010; Wei et al., 2022). Related fuzzy learning approaches have also been explored in hyperspectral image classification to address spectral variability, noise, and uncertainty, for example through fuzzy graph-based representations (Xu et al., 2024). However, in the specific context of perceptual color modeling, many traditional fuzzy approaches still require calibration from psychophysical data, which limits their scalability and integration into clinical workflows. The second paradigm builds on the theory of conceptual spaces, which model perceptual categories geometrically through prototypes, fuzzy boundaries, and Voronoi tessellation. Notably, it was introduced (Chamorro-Martínez et al., 2016) a formal framework for modeling fuzzy color

categories based on conceptual spaces, bridging the semantic gap by enabling intuitive and gradual transitions between colors. This framework laid the groundwork for the development of practical tools such as the Java-based JFCS (Soto-Hidalgo et al., 2016) and, more recently, the Python-based PyFCS library (Vazquez-Conejo et al., 2025). While prior models often lacked empirical validation or accessible implementation, the present work builds on PyFCS by delivering a usable, extensible, and domain-tailored methodology applicable to dental shade analysis.

Several recent studies have addressed uncertainty and robustness in image analysis through fuzzy and spectral-spatial learning strategies. For example, fuzzy subspace clustering has been used to improve noisy image segmentation by incorporating local and non-local information and membership-linking mechanisms (Wei et al., 2022), adaptive fuzzy weighted C-means has been combined with distance and entropy-based information for image segmentation (Song et al., 2024), fuzzy graph convolutional networks have been proposed to manage spectral variability and noise in hyperspectral image classification (Xu et al., 2024), and robust spectral-spatial residual architectures have been developed to reduce the impact of noisy labels in hyperspectral classification (Sarpong et al., 2025). These approaches mainly focus on improving segmentation or classification robustness under noise, label uncertainty, or spectral variability. In contrast, the present framework addresses uncertainty from a perceptual and semantic perspective. It models dental shades as fuzzy conceptual categories derived from prototypes and geometric relations, and produces interpretable membership distributions that can be compared with expert-based visual annotations. Therefore, the proposed approach does not aim to replace uncertainty-aware image classification methods, but rather complements them by providing a domain-specific, interpretable layer for representing perceptual ambiguity and gradual chromatic transitions in dental shade analysis.

Previous research has established a solid theoretical and computational foundation for modeling fuzzy color spaces, demonstrating the effectiveness of both parametric fuzzy set models and conceptual space-based approaches in capturing the graduality and imprecision of human color perception. Building on this foundation, the present work introduces a domain-specific extension that applies these principles specifically to the context of dental color matching. In particular, we propose the construction of a fuzzy color space aligned with the 16 shades of the VITA Classical Shade Guide, leveraging the flexibility of the PyFCS library to support interactive visualization, perceptual region analysis, and spatially-resolved pixel classification. The approach is further supported by a controlled expert-based evaluation experiment, which evaluates the system’s outputs against human assessments across defined tooth regions.

Compared with conventional instrumental methods, the proposed framework provides a perceptually grounded representation that explicitly models gradual transitions and ambiguity between neighboring shades, rather than relying solely on crisp numerical measurements. In contrast to machine learning-based dental shade-matching approaches, including support vector machines, deep learning models, and other data-driven techniques (Kim et al., 2018; Tam and Lee, 2017; Q. Li et al., 2025; Shetty et al., 2024), which often prioritize predictive accuracy and single-label classification, the proposed method yields interpretable fuzzy possibility distributions that are more closely aligned with expert reasoning in clinical shade assessment. While these approaches have demonstrated strong performance in controlled settings (Han et al., 2025; Jeong et al., 2025), they typically do not explicitly represent perceptual ambiguity or gradual transitions between neighboring color categories. Likewise, unlike many traditional fuzzy classification systems that depend on predefined or empirically tuned membership functions, the present framework derives fuzzy color categories through a geometrically grounded construction based on conceptual spaces, Voronoi partitioning, and scaling. At the same time, unlike purely predictive models evaluated on large supervised datasets, the current work is centered on perceptual interpretability and expert alignment and is not intended to demonstrate superiority over such models at this stage.

3. Preliminaries

This section outlines the theoretical and technological foundation that supports the proposed approach. First, it introduces the geometric framework of conceptual spaces and its extension to fuzzy color modeling, providing the basis for the construction of perceptually aligned categories. Next, it presents the PyFCS software library, which operationalizes this model through a modular and extensible implementation. Finally, it describes the VITA Classical Shade Guide as the reference system used in dental color selection and as the target for fuzzy color space construction in this work.

3.1. Conceptual spaces and fuzzy color modeling

The conceptual spaces framework provides a geometric model for representing knowledge based on perceptual dimensions, where concepts are encoded as convex regions in a multidimensional space (Gärdenfors, 2000). In the case of color, dimensions such as hue, chroma, and brightness form the basis of the space, and perceptual similarity is reflected by spatial proximity. This paradigm supports gradual transitions and category overlap, features that are essential for modeling perceptual categories.

To model the imprecise and graded nature of perceptual categories like color, conceptual spaces can be extended using fuzzy set theory. In this context, a fuzzy color \tilde{C} is defined in a color space C (such as RGB or CIELAB) through a membership function $\mu_{\tilde{C}} : C \rightarrow [0, 1]$, assigning to each color a continuous degree of membership. A fuzzy color space $\tilde{\Gamma}$ consists of a set of such fuzzy colors, enabling overlapping and flexible representations of colors that align with human perception (Chamorro-Martínez et al., 2016). For clarity, we distinguish between several related concepts used throughout this work. The term *perceptual color space* refers to the underlying continuous color representation (e.g., CIE-L*a*b*), whereas *fuzzy conceptual space* denotes the general conceptual framework used to model categories as fuzzy regions within perceptual domains. The term *fuzzy color space* is used more specifically to denote the set of fuzzy color categories instantiated within that framework for the dental shade analysis task.

One formal approach for constructing fuzzy color spaces builds upon the definition of positive and negative prototypes for each linguistic color term and applies a geometric partitioning method to define membership functions. The process starts by selecting a representative crisp color r_i as the prototype of a color category C_i , along with a

set of negative prototypes R_i^- associated with alternative categories. A Voronoi tessellation is then applied in the color space to generate a cell V_i around r_i , which corresponds to the 0.5-cut of the fuzzy color \tilde{C}_i . The core (V_{1i}) and support (V_{qi}) of the fuzzy set are derived by scaling this region with factors λ and λ' , which govern inclusion and separation from negative categories. Finally, membership degrees across these regions are computed by linear interpolation over the region's surfaces, yielding a smooth and perceptually grounded fuzzy representation (Chamorro-Martínez et al., 2016), as illustrated in Fig. 2.

The use of Voronoi tessellation provides a data-driven geometric partitioning of the color space, ensuring that each fuzzy category is defined in relation to its neighboring prototypes. This results in a more adaptive and perceptually consistent representation of category boundaries, since category regions are derived from the spatial distribution of colors rather than imposed through fixed thresholds. Furthermore, the application of scaling parameters to define the core and support regions introduces an additional level of flexibility, allowing the model to control the degree of overlap and separation between color categories. Together, these two mechanisms provide a principled and interpretable way of constructing fuzzy categories that remain structurally consistent while adapting to perceptual proximity relations.

This construction process provides a principled and interpretable model for fuzzy color spaces that captures key aspects of perceptual categorization, including ambiguity, graduality, and contextual dependency. These properties are especially relevant in domains such as dentistry, where color evaluation often involves subtle perceptual differences and subjective judgment.

3.2. The PyFCS library

PyFCS is an open-source Python library that implements the fuzzy color space construction model described above. It provides tools to define, manipulate, and visualize fuzzy conceptual spaces, with an emphasis on perceptual domains such as color. The library supports the definition of positive and negative prototypes, Voronoi-based partitioning, and the construction of membership functions through parametric scaling and interpolation. Color categories can be visualized in 2D and 3D, and their membership functions can be exported for use in further analysis or application.

The architecture of PyFCS is modular and extensible, making it suitable for integration into domain-specific workflows. It includes:

- A core module for defining conceptual spaces and fuzzy categories.
- A computational engine for membership evaluation and color analysis.
- A visualization module with 3D rendering of fuzzy regions.
- A graphical user interface (GUI) for interactive color space construction.

This architecture facilitates the incorporation of domain-specific components, such as tools for image-based analysis, perceptual region mapping, and validation interfaces. In this work, several such extensions have been developed and integrated into the PyFCS framework to support the application to dental shade modeling.

3.3. The VITA classical shade guide

The VITA Classical Shade Guide (Fig. 1) is a standardized tool widely used in dentistry for the selection of tooth colors in prosthetic and restorative procedures. It includes 16 discrete shades grouped into four chromatic families, each corresponding to a different perceptual hue:

- **A1, A2, A3, A3.5, A4:** Reddish-brown.
- **B1, B2, B3, B4:** Reddish-yellow.

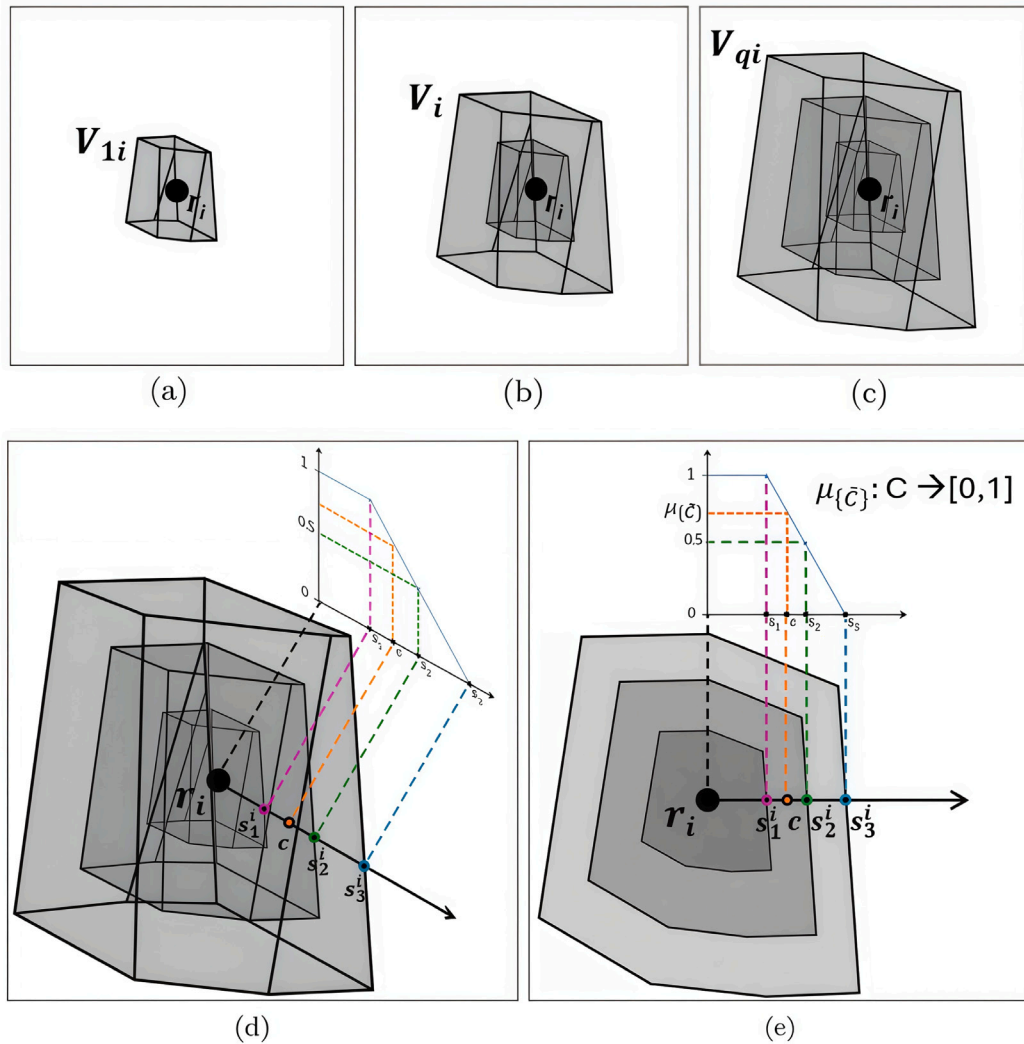


Fig. 2. Construction of fuzzy color regions around the prototype r_i . (a)–(c) sequence of polyhedral regions (V_{1i} , V_i , and V_{qi}) corresponding to the core, 0.5-cut, and support of the fuzzy color \tilde{C}_i . (d) Evaluation of a crisp color c in the 3D space and (e) its 2D projection.

- C1, C2, C3, C4: Grayish.
- D2, D3, D4: Reddish-gray.

Each shade is defined by subtle differences in hue, chroma, and lightness, and selection is typically performed by visual comparison under standardized conditions. Although widely used, the discrete and non-overlapping nature of these categories does not capture the continuous and subjective nature of color perception, often leading to variability in clinical shade selection.

The structured organization of the VITA shades, combined with their perceptual proximity and ambiguity, makes them particularly well suited for fuzzy modeling. Representing these shades as fuzzy categories within a conceptual space enables a more flexible and perceptually accurate framework, which can improve both visualization and decision-making in clinical contexts.

4. Design and implementation of the fuzzy shade matching framework

This section presents the design and implementation of a perceptually grounded framework for fuzzy color modeling in dental shade analysis. While the VITA Classical Shade Guide has been used throughout this study as a reference example, the developed framework is fully generic and adaptable to any available dental shade guide. The

contribution focuses on a domain-specific software and methodological extension of the existing PyFCS framework for dental shade analysis. Accordingly, the approach builds upon and extends the capabilities of PyFCS by incorporating four core components: (i) an interactive graphical tool for constructing fuzzy color spaces from arbitrary shade prototypes, (ii) a chromatic mapping module for pixel-wise visualization of fuzzy memberships using both grayscale and maximum-membership color renderings, (iii) a clinical region segmentation module that aggregates fuzzy distributions over a predefined 3×3 tooth region grid, and (iv) a dedicated expert evaluation interface for collecting expert-based reference annotations and evaluating system outputs. Together, these components provide a flexible and extensible framework for modeling, visualizing, and supporting the analysis of dental shade information under uncertainty.

4.1. Integration of fuzzy color space construction in PyFCS GUI

A dedicated extension has been developed and integrated into the graphical user interface (GUI) of PyFCS to enable the construction and exploration of fuzzy color spaces derived from the 16 shades of the VITA Classical Shade Guide. This integration serves a dual purpose.

First, the GUI supports the interactive creation of fuzzy color models by allowing users to input CIE-L*a*b* coordinates for each shade prototype (Fig. 3), define both positive and negative reference categories,

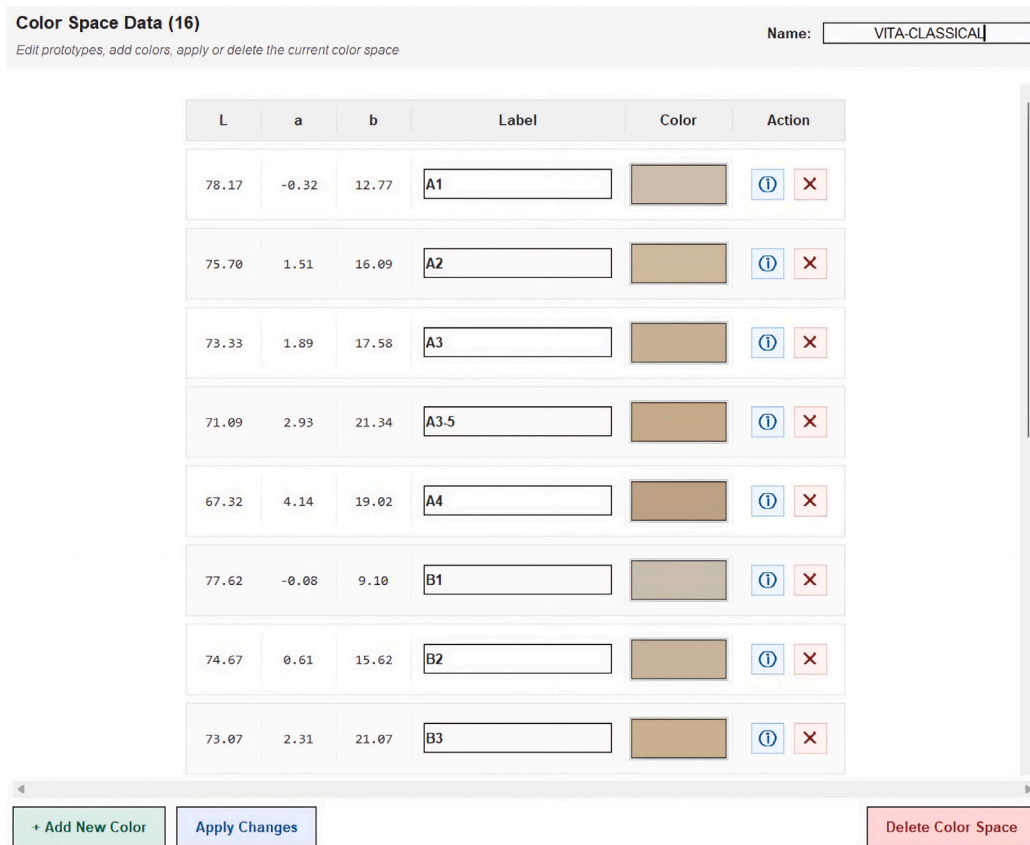


Fig. 3. Definition of the fuzzy color space \tilde{F}_{VITA} in the PyFCS GUI. Each prototype corresponds to a shade in the VITA Classical Shade Guide, specified using its CIE-L*a*b* coordinates.

and generate the corresponding fuzzy color volumes. This process adheres to the methodology established in the fuzzy conceptual space framework, including Voronoi-based tessellation and scaling to define core, α -cut (e.g., 0.5-level), and support regions. To avoid introducing non-dental categories into the fuzzy color space, background pixels are excluded through a tooth-region mask rather than represented by an additional prototype. Consequently, the fuzzy color space is defined exclusively by the dental shade categories of the VITA Classical Shade Guide.

The CIE-L*a*b* prototype values used to define the 16 shades of the VITA Classical Shade Guide were obtained experimentally through hyperspectral imaging. Specifically, each of the 16 physical shade tabs was captured using a Datacolor SpectraVision (Datacolor, 2026) system under controlled acquisition conditions. The resulting hyperspectral data were processed to derive representative CIE-L*a*b* coordinates for each shade, which were extracted from the central region of each shade tab. These experimentally derived values were then used as the reference prototypes for constructing the fuzzy color space in PyFCS, ensuring a perceptually grounded and reproducible definition of the color categories. The resulting fuzzy color space is composed of the 16 dental shades of the VITA Classical Shade Guide and is defined as $\tilde{F}_{VITA} = \{\tilde{C}_{A1}, \tilde{C}_{A2}, \dots, \tilde{C}_{D3}, \tilde{C}_{D4}\}$.

Second, the GUI offers a comprehensive and intuitive 3D visualization environment for navigating and analyzing the constructed fuzzy color space. As shown in Fig. 4, the interface includes dedicated menus for loading images, selecting shades, and managing model components. The left and central panels display the geometric volumes of each fuzzy color region — core, α -cut, and support — which can be interactively manipulated through zoom, pan, and rotation. This functionality enables detailed inspection of spatial relationships, overlaps, and distribution patterns among shades. The enhanced visualization

tools facilitate both the verification and interpretation of the fuzzy color space, aligning technical modeling with perceptual reasoning in clinical dental shade matching. The full source code is available at.¹

4.2. Chromatic mapping with spatial region segmentation

This module in PyFCS supports two complementary goals: (1) to visualize the chromatic distribution of fuzzy colors across dental images and (2) to segment anatomically relevant tooth regions for clinical evaluation.

Fuzzy visualization tools

To aid the analysis of chromatic distributions, the system introduces two types of visual outputs derived from fuzzy membership computations:

- **Grayscale Fuzzy Maps.** For each fuzzy color \tilde{C}_i , a grayscale image can be generated in which each pixel encodes its membership degree to \tilde{C}_i scaled from 0 (black, non-membership) to 255 (white, full membership). This allows a direct visual interpretation of the spatial distribution and intensity of chromatic similarity for a specific fuzzy color across the input image. For example, a pixel $p = (x, y)$ with $\mu_{\tilde{C}_i}(p) = 0.5$ will be rendered as a medium gray (value 128), while $\mu_{\tilde{C}_i}(p) = 1.0$ will appear as pure white (value 255). This method provides a smooth visual gradient that intuitively reflects perceptual degrees of match.

¹ https://github.com/RafaelConejo/PyFCS_DentalShades

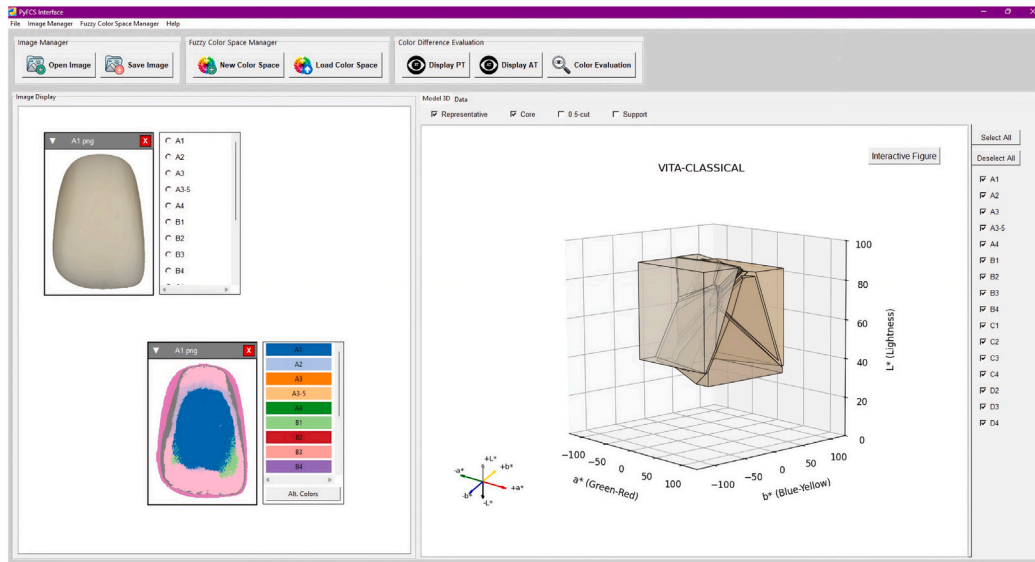


Fig. 4. Graphical User Interface (GUI) in PyFCS for VITA Classical Shade Guide.

- Chromatic Mapping.** To obtain an overall chromatic interpretation of a dental image, the system computes the membership degree of each pixel $p = (x, y)$ to all fuzzy colors $\tilde{C}_i \in \tilde{F}$, and assigns to it the color of the fuzzy category with the highest membership. This *winner-takes-all* strategy yields a categorical mapping that emphasizes the dominant chromatic association per pixel.

Formally, for a given pixel p , we define the fuzzy membership distribution over the color space as:

$$\tilde{F}(p) = \left\{ \mu_{\tilde{C}_i}(p) / \tilde{C}_i \mid \mu_{\tilde{C}_i}(p) > 0, \tilde{C}_i \in \tilde{F} \right\}$$

where $\mu_{\tilde{C}_i}(p) \in [0, 1]$ denotes the degree of membership of pixel p to the fuzzy color \tilde{C}_i . The pixel is then assigned the color of the fuzzy category with maximum membership:

$$\tilde{C}_{\max} = \arg \max_{\tilde{C}_i \in \tilde{F}} \mu_{\tilde{C}_i}(p)$$

For example, if the membership distribution is:

$$\tilde{F}_{\text{VITA}}(p) = 0.6 / \tilde{C}_{A1} + 0.4 / \tilde{C}_{A3}$$

then the pixel p is mapped to the color associated with \tilde{C}_{A1} , since it has the highest membership.

In cases where multiple fuzzy colors share the maximum membership value (i.e., a tie), the system selects the first occurrence according to the predefined color ordering. This behavior is configurable, allowing the use of alternative tie-breaking strategies if required.

This classification process is applied to all pixels in the input image, generating a complete color segmentation map based on the dominant fuzzy shade per pixel.

To improve interpretability in cases where the fuzzy shades might be perceptually similar — as is common with the 16 VITA Classical shades — the graphical user interface includes an optional visualization mode. This mode remaps each fuzzy category to a clearly distinguishable color for display purposes. It is important to note that this remapping is purely visual and does not alter the underlying fuzzy classification logic.

Fig. 5 shows an example grayscale fuzzy map for the A1 shade, while Fig. 6 displays the corresponding full color-coded chromatic mapping. Two visualization strategies are illustrated: (a) a high-contrast color palette that enhances the perceptual distinction between fuzzy color categories, and (b) the use of representative colors corresponding to each fuzzy category as defined in the original VITA Classical Shade Guide.

Fig. 7 summarizes these visualization modalities by comparing grayscale and chromatic mappings across different samples (A1 and B2).

These visualizations should be interpreted as qualitative tools for inspecting the spatial distribution of fuzzy memberships and dominant shade assignments. They are not intended, by themselves, to constitute evidence of clinical correctness; quantitative assessment is performed separately through region-wise comparison with expert-based reference annotations.

4.3. Clinical region segmentation

To support region-specific chromatic analysis, the developed framework includes a module for segmenting the input image into a clinically meaningful 3×3 grid. This grid is applied after excluding background pixels from the tooth image rather than to the full rectangular image indiscriminately. It provides an operational approximation of the cervical, middle, and incisal thirds, together with left, central, and right sectors, over the visible crown area. Regional fuzzy possibility distributions are computed only from valid tooth pixels. Background pixels are excluded from the aggregation process and are not assigned to any dental shade category. Therefore, non-dental image areas do not contribute to the estimated regional shade distributions.

Each cell of the grid corresponds to an anatomical subregion of the tooth: incisal, middle, and cervical thirds along the vertical axis, and left, center, and right sectors horizontally (mesio-distal axis). This design choice provides a standardized and reproducible spatial reference for the controlled expert-evaluation study. It is consistent with clinical shade assessment practice, where cervical, middle, and incisal regions are commonly estimated visually and proportionally over the crown surface rather than delimited by universal anatomical lines. The use of symmetric horizontal and vertical divisions also facilitated the expert annotation task, since each region could be identified consistently across samples during the visual evaluation.

For each of the nine segmented regions, a fuzzy possibility distribution is computed over the color space \tilde{F} . Since the fuzzy memberships $\mu_{\tilde{C}_i}(p) \in [0, 1]$ are defined at the pixel level for every fuzzy color $\tilde{C}_i \in \tilde{F}$, the regional aggregation requires combining the pixel-wise information across the region $R \subseteq \text{Image}$ into a single distribution. Two aggregation strategies are supported in our system:

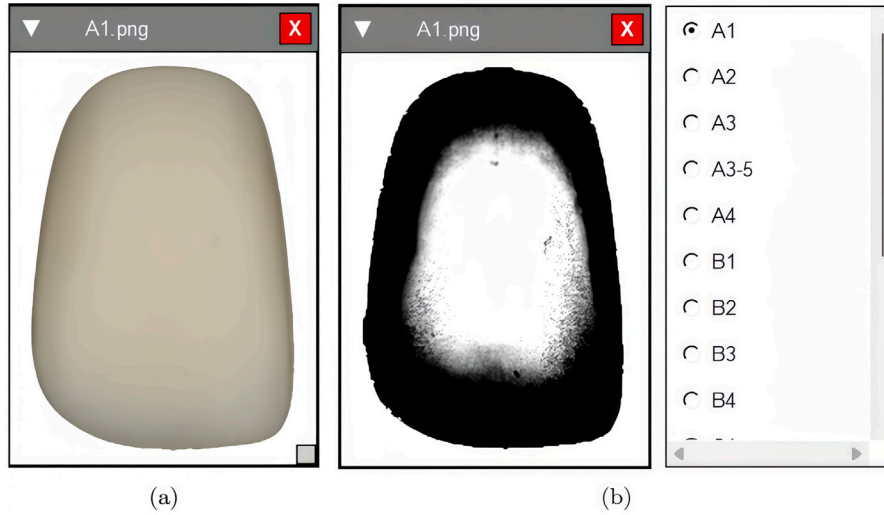


Fig. 5. (a) Standard color image of a tooth corresponding to shade A1. (b) Grayscale fuzzy membership map derived from the same image, tooth A1. Pixel values represent degrees of membership scaled from 0 to 255.

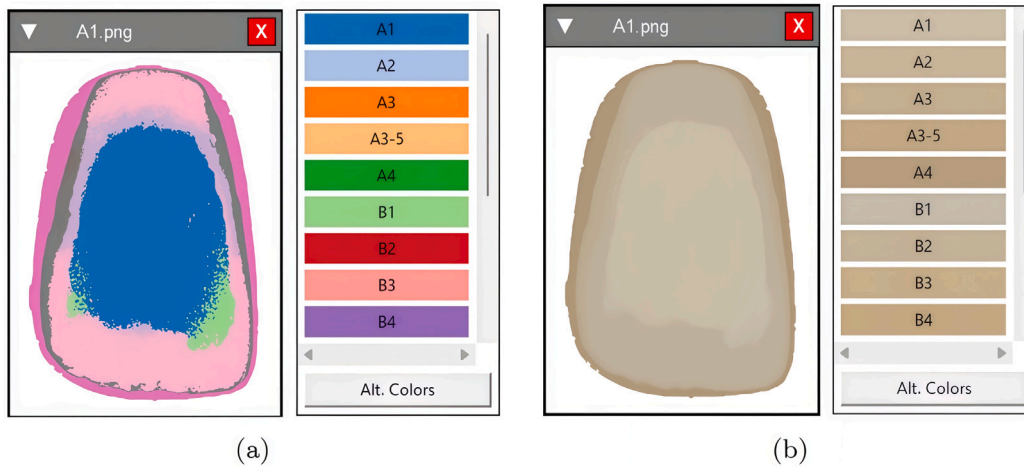


Fig. 6. Chromatic mapping outputs for a dental sample annotated as A1. (a) Mapping using a high-contrast visualization palette to enhance the distinction between fuzzy color categories. (b) Mapping using the representative colors of each fuzzy category based on the original VITA Classical shade guide.

4.3.1. Max-possibility aggregation

For each fuzzy color $\tilde{C}_i \in \tilde{\Gamma}$ and a given region $R \subseteq \text{Image}$, the Max-Possibility Aggregation $\tilde{\Gamma}_{max}$ strategy computes the highest membership degree among all pixels in R with respect to \tilde{C}_i . Formally, the aggregated membership for the region is defined as:

$$\mu_{\tilde{C}_i}^{(R)} = \max_{p \in R} \mu_{\tilde{C}_i}(p) \quad (1)$$

This results in a possibility distribution over the fuzzy color space:

$$\tilde{\Gamma}_{max}(R) = \mu_{\tilde{C}_1}^{(R)} / \tilde{C}_1 + \mu_{\tilde{C}_2}^{(R)} / \tilde{C}_2 + \dots + \mu_{\tilde{C}_n}^{(R)} / \tilde{C}_n \quad (2)$$

This approach highlights the most prominent fuzzy shade present in the region, enabling the detection of dominant chromatic patterns.

This method offers the advantage of identifying sharp or localized chromatic signals, making it particularly suitable when the goal is to detect high-confidence shade occurrences. However, its main limitation lies in its extreme sensitivity to outliers—i.e., a single pixel with a high membership value can disproportionately affect the entire region's representation, even if the rest of the region shows little or no affiliation to that shade. This sensitivity can lead to misleading interpretations in cases where spurious values are present due to noise, reflections, or segmentation artifacts.

4.3.2. Normalized average aggregation

Given a fuzzy color $\tilde{C}_i \in \tilde{\Gamma}$ and a region $R \subseteq \text{Image}$, the Normalized Average Aggregation $\tilde{\Gamma}_{avg}$ computes the average membership of all pixels in the region to \tilde{C}_i , and then normalizes the resulting values so they sum to 1, producing a valid possibility distribution. Formally, the raw average is given by:

$$\bar{\mu}_{\tilde{C}_i}^{(R)} = \frac{1}{|R|} \sum_{p \in R} \mu_{\tilde{C}_i}(p) \quad (3)$$

Then, the normalized possibility distribution for the region is obtained as:

$$\mu_{\tilde{C}_i}^{(R)} = \frac{\bar{\mu}_{\tilde{C}_i}^{(R)}}{\sum_{j=1}^n \bar{\mu}_{\tilde{C}_j}^{(R)}} \quad (4)$$

$$\tilde{\Gamma}_{avg}(R) = \mu_{\tilde{C}_1}^{(R)} / \tilde{C}_1 + \mu_{\tilde{C}_2}^{(R)} / \tilde{C}_2 + \dots + \mu_{\tilde{C}_n}^{(R)} / \tilde{C}_n \quad (5)$$

This method provides a smoothed representation of the overall chromatic composition of the region, mitigating the impact of isolated pixel anomalies.

One key advantage of this aggregation strategy is its robustness to outliers, as it reflects the collective chromatic tendencies of all pixels in the region. It is especially suitable when regional shade characterization requires a global and balanced summary. However, a potential

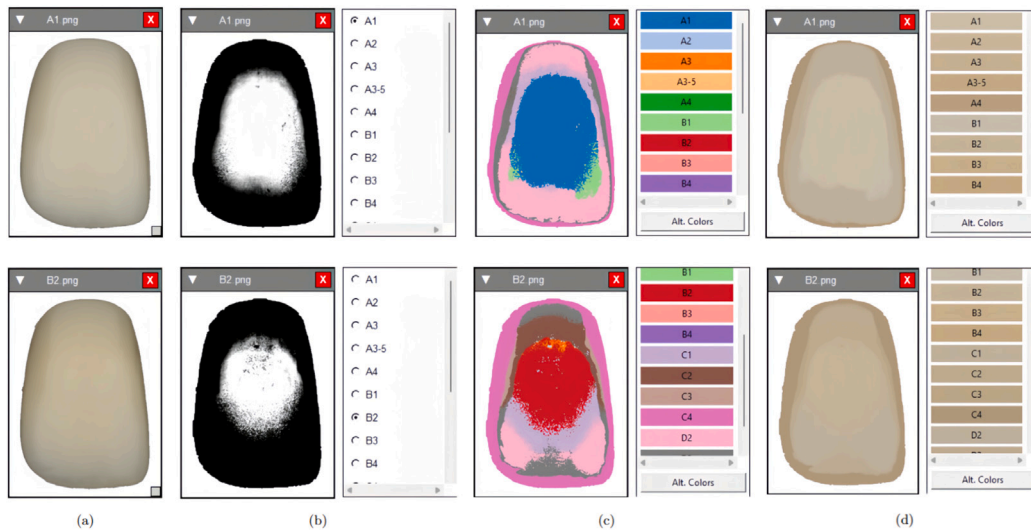


Fig. 7. Comparison of visual outputs generated by the proposed framework for representative dental samples (A1 and B2). (a) Original tooth images. (b) Grayscale fuzzy membership maps, where pixel intensity represents the degree of membership to the selected fuzzy color. (c) Chromatic mappings using a high-contrast visualization palette to enhance the distinction between fuzzy color categories. (d) Chromatic mappings using the representative colors associated with each shade in the VITA Classical Shade Guide. This comparison illustrates how fuzzy memberships are translated into spatially interpretable color representations under different visualization strategies.

drawback is that highly dominant but spatially localized shades may be underrepresented if their presence is diluted by the averaging process across a large region.

4.3.3. Implementation in PyFCS

Both aggregation strategies — Max-Possibility Aggregation and Normalized Average Aggregation — have been fully integrated into the PyFCS graphical interface as part of the region-based analysis module. Users can interactively enable segmentation of the clinical region by overlaying a predefined 3×3 grid on the input image, dividing the area of the tooth into nine anatomically relevant zones: the incisal, middle and cervical thirds, further subdivided into left, center and right (mesio-distal) segments.

For each segmented region, the system computes a fuzzy possibility distribution over the color space using the selected aggregation method. A dedicated selector within the GUI allows users to switch between the two strategies:

- **Max-Possibility Aggregation** highlights the strongest observed associations between any pixel and each fuzzy color, revealing dominant shades that might be localized or spatially sparse.
- **Normalized Average Aggregation** delivers a smoother representation by integrating all pixel memberships and normalizing the result, offering a more stable regional chromatic profile.

The results are displayed in real-time for each of the nine regions as fuzzy possibility distributions in textual format. Specifically, each region is associated with a distribution expressed as a sequence of graded memberships:

$$\mu_1/\tilde{C}_1 + \mu_2/\tilde{C}_2 + \dots + \mu_k/\tilde{C}_k$$

where $\mu_i \in [0, 1]$ denotes the degree of membership of the region to the fuzzy color \tilde{C}_i . These distributions can be exported in machine-readable formats such as JSON and CSV, enabling further integration into external analysis workflows.

Examples of these region-based outputs are illustrated in Figs. 8 and 9. Each figure presents the possibility distributions computed for the nine tooth regions using the implemented aggregation strategies—maximum membership and normalized average. These outputs provide clinicians with interpretable summaries of the chromatic structure on dental surfaces.

4.4. Expert evaluation interface

To facilitate expert-driven assessment of shade predictions, a specialized evaluation module has been developed and integrated into the graphical user interface (GUI) of PyFCS. This tool enables structured visual evaluation of dental samples by experts, offering both intuitive interaction and standardized annotation.

As illustrated in Fig. 10, the top bar of the interface displays all 16 shades of the VITA Classical Shade Guide. These digital shade tabs can be selected and dragged toward the central panel, where a dental sample is shown alongside its reference color, allowing direct visual comparison between the real and reconstructed samples. Users can toggle between “Reference Tooth” and “Reference Color” modes to adjust the comparison context.

The core of the interface is the region-based evaluation panel, where the tooth is divided into three anatomical zones: cervical, middle, and incisal thirds. For each region, the expert can:

- **Assign multiple shades:** Up to three shade categories can be selected from a dropdown menu, corresponding to the fuzzy colors defined in the fuzzy color space \tilde{I}_{VITA} .
- **Score membership degrees:** For each selected shade, a numerical degree of membership $\mu_{\tilde{C}_i} \in [0, 1]$ is assigned via a slider or text input. These values reflect the perceived association of the expert between the region and each fuzzy color.
- **Real-time feedback:** The selected fuzzy color’s representative RGB value is displayed above each input field, offering immediate visual feedback and assisting in perceptual confirmation.

Effectively, this interface enables the construction of a possibility distribution over fuzzy color categories for each region of the tooth, structured as:

$$\tilde{I}_{Expert}^{(R)} = \mu_{Expert_{\tilde{C}_i}^{(R)}}/\tilde{C}_i + \mu_{Expert_{\tilde{C}_j}^{(R)}}/\tilde{C}_j + \mu_{Expert_{\tilde{C}_k}^{(R)}}/\tilde{C}_k$$

where R is the region $R \in \{\text{upper, middle, lower}\}$ and each $\mu_{Expert_{\tilde{C}_x}^{(R)}} > 0$ corresponds to an expert-assigned membership value for that region and color. This representation mirrors the fuzzy distribution obtained through the automated PyFCS pipeline, enabling direct comparison during the evaluation phase.

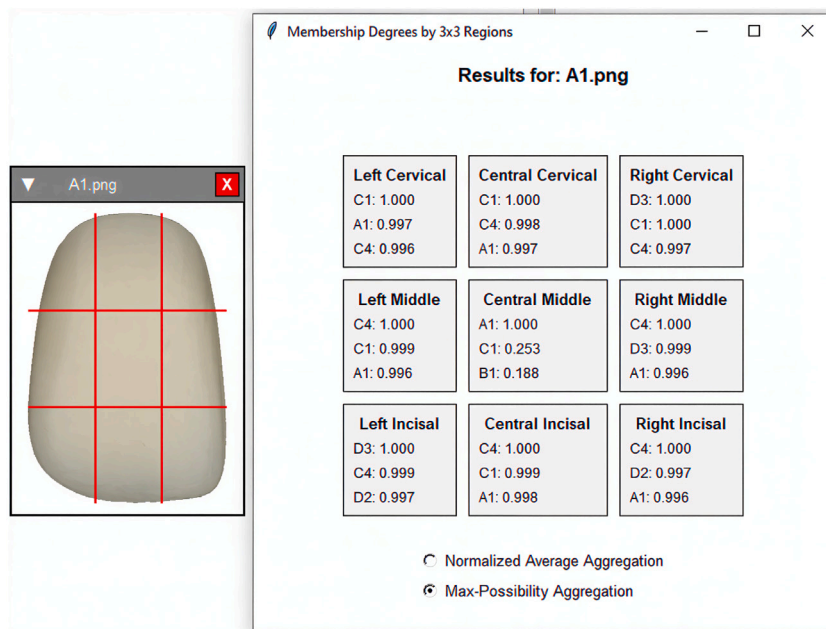


Fig. 8. Region-based fuzzy possibility distributions using the *maximum membership* aggregation strategy. Each region (1 to 9) displays the dominant fuzzy shades identified, along with their corresponding membership degrees.

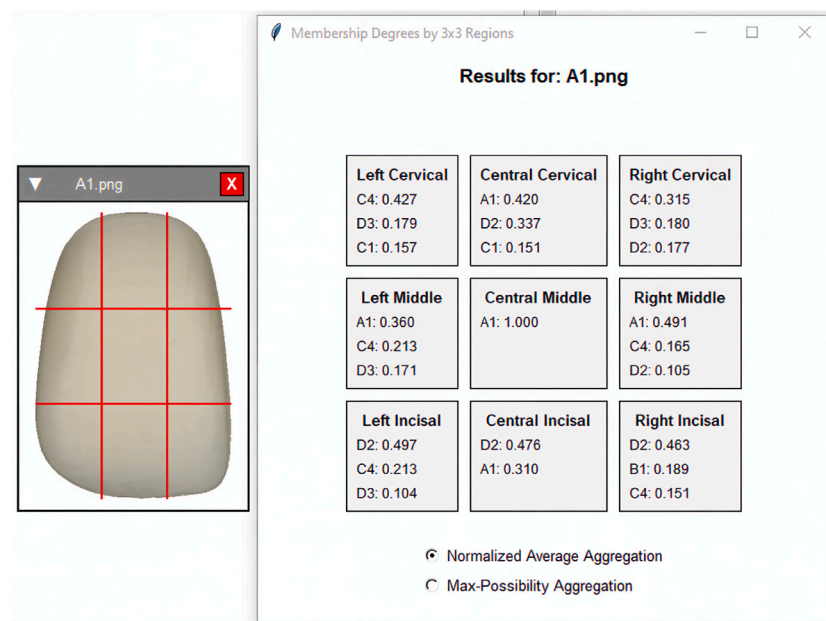


Fig. 9. Region-based fuzzy possibility distributions using the *normalized average* aggregation strategy. Possibility distributions reflect the averaged memberships of all pixels within each region, providing a smoother characterization of shade dominance.

At the bottom of the interface, the navigation buttons allow experts to move through the full set of images (16 samples), reset the annotations, and toggle the comparison modes. All inputs are stored in a structured format for further analysis.

The evaluation module is fully integrated into the PyFCS ecosystem and is available as part of the open-source repository,² which

includes complete documentation and usage instructions. Implemented in Python using the Tkinter framework, it supports reproducible evaluation workflows and seamless data integration with the fuzzy reasoning core.

4.5. Practical integration with dental imaging workflows

From a practical implementation perspective, PyFCS can be incorporated into existing dental imaging workflows as an interpretative layer

² https://github.com/RafaelConejo/PyFCS_DentalShades

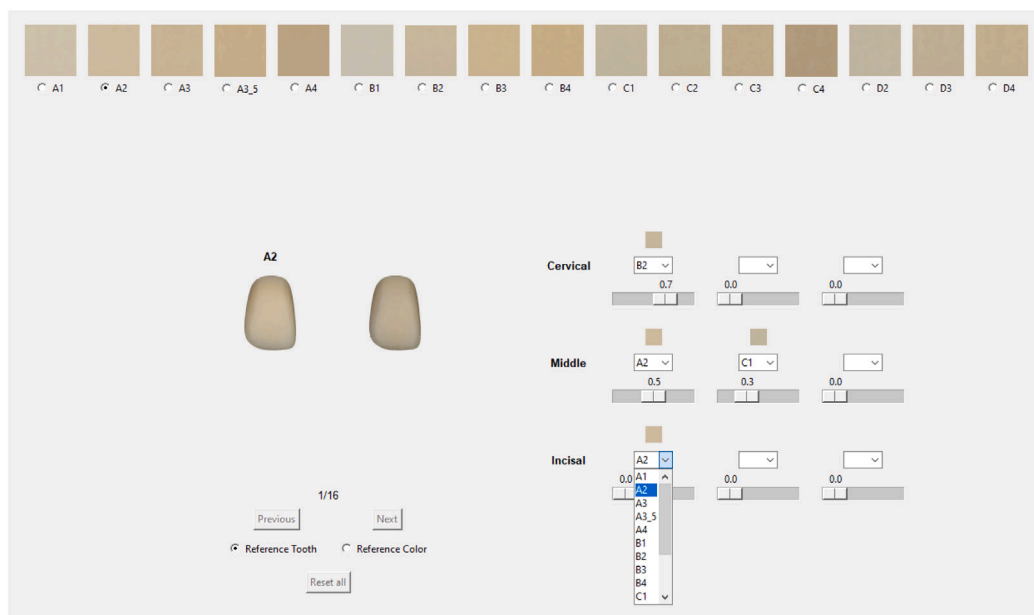


Fig. 10. Expert evaluation interface integrated into PyFCS. The top panel contains the 16 VITA Classical shades, while the central area shows the sample under evaluation. The lower panel allows region-wise shade selection and confidence scoring across upper, middle, and lower thirds of the tooth.

rather than as a replacement for acquisition devices. Calibrated color information obtained from digital photography, spectrophotometric devices, intraoral scanners, or similar systems can be converted into CIE-L*a*b* coordinates and subsequently processed by the framework to compute pixel-wise fuzzy memberships, generate chromatic maps, and derive region-wise fuzzy possibility distributions.

5. Expert evaluation protocol

This section presents the experimental protocol designed to assess the expert alignment and interpretability of the proposed fuzzy conceptual space framework for dental shade analysis under controlled conditions. The evaluation was carried out through a structured methodology involving qualified dental professionals who used the PyFCS interface to annotate chromatic distributions in standardized dental samples.

To ensure methodological rigor, the protocol was divided into several stages. First, we describe the selection of participants and the materials used in the study. Next, we outline the annotation procedure performed through the graphical interface and detail the specific experimental conditions under which the study was conducted. All interactions and annotations were recorded for subsequent analysis. To quantify the agreement between expert annotations and system outputs, we applied the fuzzy Jaccard similarity metric, which allows comparison between possibility distributions over fuzzy shade categories. The following subsections provide a comprehensive account of each component of the evaluation protocol.

Participants and materials

Twelve dental professionals with proven experience in clinical shade matching participated in the study. All participants had a minimum of five years of clinical practice and prior training in the use of the VITA Classical Shade Guide. Each expert received a full set of 16 digital dental sample images, each corresponding to one of the VITA Classical shades.

These reference samples were rendered in high resolution under standardized lighting on a color calibrated display and derived from validated photographic datasets commonly used in dental color research.

Interface and annotation task

The evaluation was carried out using the integrated validation interface within PyFCS (Section 4.4). Since visual experiments should not be excessively long due to attention span and visual fatigue constraints, the expert evaluation was limited to the central regions of the teeth. These regions were considered sufficient to support meaningful conclusions without requiring excessively long experimental sessions. Accordingly, for each image, experts were asked to evaluate the chromatic composition of the tooth across three anatomical regions: central cervical, central middle, and central incisal thirds.

For each region, they were required to:

- Select up to three VITA shades from the predefined fuzzy color space.
- Assign a membership degree $\mu \in [0, 1]$ to each selected shade, reflecting the perceived degree of correspondence with the observed chromatic appearance.

Experts were instructed to select the shades they considered visually compatible with each evaluated region and to assign higher membership degrees to those perceived as more representative of the observed chromatic appearance. The assigned values were therefore interpreted as relative degrees of perceptual compatibility within each expert's annotation for a given region, rather than as absolute psychometric confidence scores. In practical terms, values close to 1 indicated a shade perceived as highly representative of the region, intermediate values reflected partial compatibility or transitional appearance, and values close to 0 indicated weak or negligible compatibility. When the appearance of a region was judged to be ambiguous or transitional, multiple shades could be selected with different membership degrees in order to reflect this uncertainty. Although this procedure was designed to capture expert perceptual judgment in a flexible manner, it is inherently subject to inter-observer variability and potential perceptual biases. To mitigate these effects, all evaluations were performed under standardized viewing conditions using calibrated displays, a common annotation interface, and a controlled visual environment.

Experimental conditions

All evaluations were conducted in a fully light-controlled environment, free from ambient light and external visual interference.

The assessments were performed using a calibrated monitor, with the following specifications:

- **Device calibration:** the monitors were calibrated using a Calibrite Display Pro HL colorimeter in accordance with ISO 3664:2009 standards for color-critical viewing in graphic arts and medical imaging.
- **Luminance and chromatic fidelity:** Screen brightness was standardized at $120 \text{ cd/m}^2 \pm 5\%$, and chromatic deviations were maintained within a ΔE threshold of < 1.0 to ensure imperceptibility under clinical conditions (Paravina et al., 2019).
- **Viewing geometry:** Monitors were positioned at eye level with a 90-degree viewing angle and a fixed observer distance of 50 cm, consistent with clinical protocols.

Each participant completed the evaluation of all 16 samples in a single session. No time limits were imposed, allowing experts to perform thorough and reflective assessments without external pressure.

Data recording and usage

All annotations were recorded in a structured format, preserving:

- The image ID and true reference shade.
- For each anatomical region: the selected shades, their membership degrees, and their ordering.

These expert distributions served as expert-based reference annotations, rather than as absolute numerical ground truth, for comparison with the fuzzy chromatic outputs generated by PyFCS. The use of possibility distributions in both expert annotations and system predictions allows a direct evaluation of perceptual alignment through fuzzy similarity metrics, such as the fuzzy Jaccard similarity metric (see Section 6).

Fuzzy similarity measurement

To assess the degree of agreement between the fuzzy shade predictions generated by PyFCS and the visual assessments made by dental experts, the *fuzzy Jaccard similarity* metric was used. This similarity measure, widely adopted in fuzzy set theory, quantifies the overlap between two fuzzy sets by comparing their membership distributions.

Given two fuzzy sets A and B , the fuzzy Jaccard similarity is computed as:

$$J(A, B) = \frac{\sum_i \min(A_i, B_i)}{\sum_i \max(A_i, B_i)}$$

where A_i and B_i denote the membership degrees of element i in the respective sets. The resulting value lies in the interval $[0, 1]$, where 0 indicates no overlap and 1 indicates perfect agreement.

In the revised evaluation, total disagreement cases were retained and assigned a Jaccard similarity of 0, so the primary metric is the full fuzzy Jaccard similarity computed over both overlapping and non-overlapping cases. This explicitly penalizes cases in which PyFCS and the experts selected completely different shades. A secondary partial-overlap analysis, excluding zero-overlap cases, is also reported to describe the degree of similarity when at least some shade overlap exists, together with the complete-disagreement rate for each anatomical region.

6. Results and discussion

This section presents the experimental findings obtained by comparing the fuzzy shade assignments produced by PyFCS with expert-based reference annotations collected through the evaluation interface. The objective is to quantify the agreement between system predictions and human judgment using a perceptually grounded similarity metric, and to analyze the consistency of the proposed approach across different anatomical regions of the tooth. The full fuzzy Jaccard similarity is

reported as the primary metric, complemented by the partial-overlap Jaccard and the complete-disagreement rate. The results are organized into two parts: (i) regional agreement analysis, and (ii) clinical interpretation and implications of the findings.

6.1. Agreement across anatomical tooth regions

Following the completion of the visual shade matching task by twelve expert participants, the performance of PyFCS was quantitatively evaluated using the full fuzzy Jaccard similarity as the primary metric.

Fig. 11 shows the distribution of full Jaccard similarity scores for each of the three assessed regions: cervical (upper third), middle (central third), and incisal (lower third). The boxplot depicts medians, interquartile ranges, and outlier values, allowing comparative assessment of system-expert agreement when zero-overlap cases are included. Fig. 12 reports the corresponding partial-overlap analysis as a complementary visualization.

The highest agreement was observed in the middle third, which is traditionally considered the most clinically relevant region for shade matching. Using the full Jaccard similarity, this region reached a mean value of 0.68 ± 0.30 , with a median of 0.75, and complete disagreement occurred in only 10.4% of evaluations. When only partial-overlap cases were considered, the mean similarity was 0.76 ± 0.20 , very close to the value reported in the previous analysis. This indicates that the inclusion of zero-overlap cases has a comparatively limited effect on the middle region, where system-expert overlap was generally preserved.

Notably, within the VITA Classical-based experimental setting, the dominant fuzzy shade predicted by PyFCS was consistent with the nominal reference shade of the evaluated samples. However, this result should be interpreted as evidence of internal consistency and expert alignment within the constructed VITA reference space, rather than as a definitive validation of clinical tooth shade recognition on independent natural teeth.

In contrast, the cervical third exhibited lower agreement when total disagreements were included, with a full Jaccard similarity of 0.43 ± 0.32 and a median of 0.47. Complete disagreement occurred in 26.6% of evaluations. In the secondary partial-overlap analysis, the similarity increased to 0.58 ± 0.21 , suggesting that the difference between full and partial scores is mainly driven by zero-overlap cases. This reduction is consistent with the more pronounced chromatic gradients and shadows in this region, which complicate both human and algorithmic assessment.

The incisal third showed the greatest variability and the lowest full Jaccard similarity, with a mean value of 0.34 ± 0.34 and a median of 0.31. Complete disagreement was observed in 40.1% of evaluations, the highest rate among the three regions. When zero-overlap cases were excluded in the secondary partial-overlap analysis, the similarity increased to 0.57 ± 0.24 . This pattern indicates that excluding zero-overlap cases mainly affects the cervical and incisal regions, where complete disagreements are more frequent, and allows the partial-overlap analysis to describe the degree of similarity only when some shade overlap exists. The higher variability in the incisal third is consistent with its greater translucency and lower chromatic saturation, which introduce additional ambiguity in visual evaluations, as was also demonstrated in Tejada-Casado et al. (2024).

6.2. Interpretation and clinical implications

The comparatively higher agreement observed in the middle third suggests the potential of PyFCS to support interpretable shade analysis under controlled conditions, while the lower values in the cervical and incisal regions highlight the need for cautious interpretation. The system's use of perceptually motivated fuzzy representations may help represent chromatic transitions and category overlap in a way that is consistent with expert reasoning.

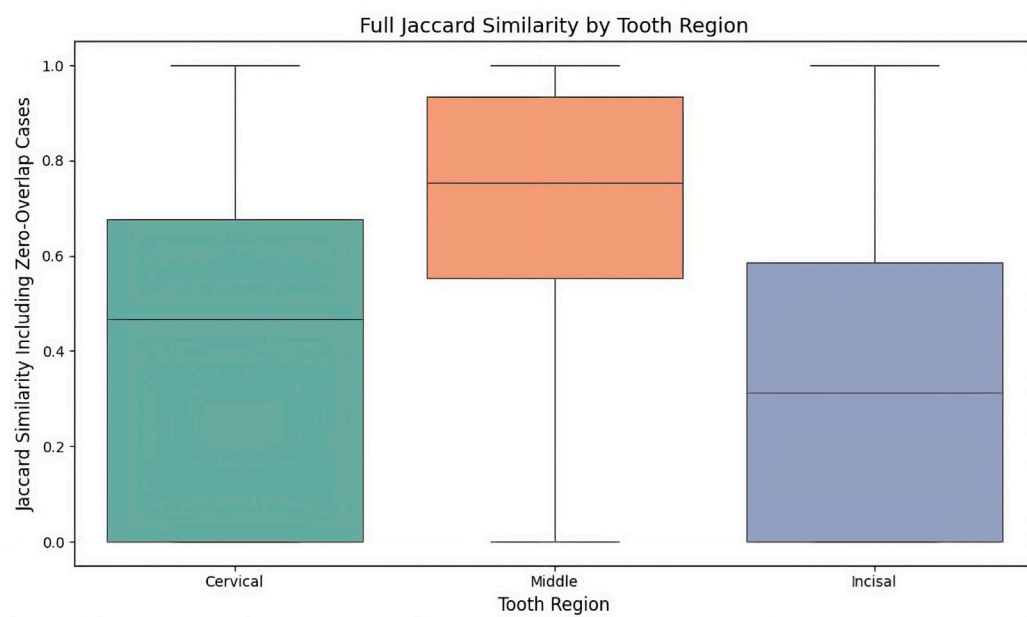


Fig. 11. Boxplot of full fuzzy Jaccard similarity scores across the cervical, middle, and incisal thirds. Zero-overlap cases are included and assigned a Jaccard similarity of 0.

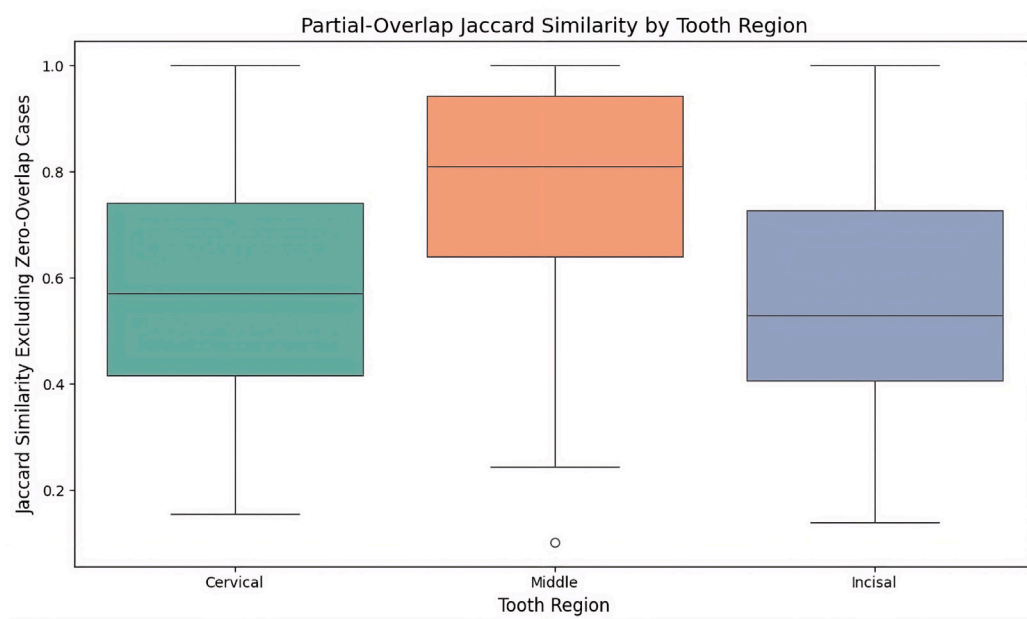


Fig. 12. Boxplot of partial-overlap fuzzy Jaccard similarity scores across the cervical, middle, and incisal thirds. Zero-overlap cases are excluded in this secondary analysis.

These differences can be interpreted in light of known clinical and perceptual characteristics of the tooth. The middle third is generally considered the most reliable region for shade selection, as it exhibits more stable and representative chromatic properties. In contrast, the cervical region is influenced by gingival tissues and shadowing effects, while the incisal third presents additional challenges due to its higher translucency and lower chromatic saturation, which reduce the reliability of direct color measurements (Ahmed et al., 2024).

From a clinical standpoint, these discrepancies also have different levels of impact. Errors in the middle third are typically more critical

for overall aesthetic perception, as this region largely determines the perceived tooth color. In comparison, variations in the incisal region may be less perceptually dominant due to its translucent nature, although they remain relevant for high-quality aesthetic restorations. Therefore, lower agreement in the cervical or incisal regions should not be assumed to have the same clinical relevance as an equivalent discrepancy in the middle third, since each region contributes differently to the overall perceptual outcome and to restorative decision-making.

One of the main practical strengths of the system is its adaptability. Although this evaluation used predefined CIE-L*a*b* values from

the VITA Classical Shade Guide, PyFCS allows users to recalibrate these prototypes to match institutional standards, device characteristics, or clinician preferences, without compromising the consistency and reproducibility of the underlying model.

In real clinical practice, image acquisition is often affected by variability in illumination conditions, camera settings, viewing geometry, and specular reflections. Although standardized acquisition protocols are desirable, they cannot always be guaranteed. In this context, PyFCS can be adapted to the specific acquisition conditions of each setting by recalibrating the fuzzy color space from user-defined prototypes. This flexibility also facilitates its integration with existing dental imaging systems, since calibrated color information obtained from digital photography, spectrophotometric devices, or intraoral scanners can be incorporated into the same perceptually grounded analysis framework.

Within the controlled and exploratory scope of the present study, the fuzzy possibility distributions generated by PyFCS may be interpreted as exploratory decision-support profiles for restoration planning research, rather than as clinically validated prescriptions for material selection. In future clinical-oriented or laboratory-oriented implementations, the shade with the highest membership degree could serve as the primary reference for material selection, similarly to conventional shade-matching procedures. At the same time, the distribution of memberships across multiple shades provides additional information about chromatic transitions and spatial variability, particularly in adjacent regions. In practical laboratory use, this output should be interpreted as a decision-support profile rather than as a single mandatory shade assignment: when one shade is clearly dominant, it can guide the main material selection, whereas relevant secondary memberships may indicate the need for stratified characterization, intermediate transitions, or region-specific adjustments in the restoration. This information may be especially useful in layered restorations, where reproducing the natural heterogeneity of dental tissues is essential for achieving more accurate and region-specific color reconstruction.

Furthermore, because the system allows the use of user-defined CIE-L*a*b* prototypes, it can be adjusted to the calibration procedures, working conditions, and interpretative preferences of a given laboratory, which facilitates the translation of fuzzy outputs into concrete fabrication decisions. In this way, the output does not replace the technician's expertise, but provides a structured representation of chromatic dominance and ambiguity that can support more informed fabrication decisions.

The proposed framework may be particularly valuable in cases where tooth color cannot be adequately represented by a single discrete shade label, such as teeth with gradual chromatic transitions, localized characterizations, or marked regional heterogeneity. In such scenarios, the use of fuzzy possibility distributions can provide a more informative basis for restoration planning and clinician-technician communication than conventional single-shade assignments. By supporting a more explicit representation of chromatic ambiguity and spatial variation, the framework may provide a useful basis for future studies on clinician-technician communication and restoration planning workflows. However, its impact on aesthetic predictability, treatment outcomes, patient satisfaction, or workflow efficiency remains to be evaluated in real clinical settings.

In this context, the two aggregation strategies implemented in the system can support complementary analytical objectives. Max-Possibility aggregation is more suitable when the goal is to detect localized chromatic variations or small but perceptually relevant shade components, whereas Normalized Average aggregation is better suited for obtaining a balanced characterization of the overall regional shade, which may be more useful for general restoration planning.

Overall, the results suggest that PyFCS provides a promising and perceptually aligned basis for interpretable shade analysis within the controlled setting evaluated in this study, especially in regions where expert agreement is higher and the need for standardization is critical (see Table 1).

Table 1

Summary of full and partial-overlap Jaccard similarity across anatomical tooth regions. Full Jaccard includes zero-overlap cases, whereas partial-overlap Jaccard is computed only over cases with non-zero overlap. Each region includes 192 evaluations, corresponding to 16 images assessed by 12 experts.

Tooth region	Full Jaccard	Partial-overlap Jaccard	Complete disagreement
Cervical	0.43 ± 0.32	0.58 ± 0.21	26.6%
Middle	0.68 ± 0.30	0.76 ± 0.20	10.4%
Incisal	0.34 ± 0.34	0.57 ± 0.24	40.1%

7. Limitations and future work

The present study was conducted under controlled imaging conditions, including standardized illumination and calibrated acquisition devices. While this setup supports reproducibility and reliability, it does not fully reflect the variability encountered in real clinical environments. In practice, factors such as non-uniform lighting, device heterogeneity, viewing geometry, saliva, and specular reflections may affect the quality and consistency of color acquisition. For this reason, a clinically appropriate acquisition protocol should aim to reduce uncontrolled illumination changes, maintain consistent camera settings and viewing geometry, and minimize saliva and specular reflections whenever possible. In this context, the use of calibrated imaging devices, controlled lighting conditions, and standardized positioning is recommended. However, the current version of the framework has not yet been systematically evaluated on non-ideal clinical images acquired under such variable conditions. An important next step will therefore be the assessment of the robustness of the proposed framework under less controlled, real-world settings. Accordingly, the present study should be interpreted as a controlled expert-based evaluation of the proposed software framework, rather than as evidence of clinical shade-matching performance under real intraoral conditions.

As with any perceptual evaluation, the annotation process is inherently subject to inter-observer variability and potential biases related to individual visual perception. These factors may influence the consistency of expert annotations, particularly in regions with higher chromatic ambiguity. In this respect, the use of fuzzy possibility distributions provides a flexible representation that naturally accommodates uncertainty and variability in expert judgments, although broader validation will still be necessary to further consolidate the framework. Therefore, the fuzzy Jaccard similarity should be interpreted as a measure of distributional overlap with expert-based annotations, rather than as evidence that all experts used the numerical membership scale in an identical or formally calibrated way. Future studies should further strengthen the expert annotation protocol through calibration training, repeated annotations, and inter-rater reliability analysis, in order to assess more precisely how consistently experts use the membership scale.

Although this study has focused on the VITA Classical Shade Guide, the PyFCS framework is not restricted to this system and can be configured to represent alternative shade guides and recalibrated to reflect different acquisition settings. It should also be noted that the present evaluation remains internal to the VITA Classical reference system. Although the fuzzy prototypes were obtained from hyperspectral measurements of central regions of physical shade tabs and the evaluated samples involved spatially distributed tooth representations rather than the same prototype coordinates, this setup does not constitute an external validation on independent natural teeth. Therefore, the reported results should be interpreted as evidence of internal consistency and expert alignment within the constructed VITA reference space, rather than as a definitive validation of generalized clinical tooth shade recognition. Future research will therefore explore the application of the method to more densely populated shade guides, as well as its validation on larger and more diverse datasets, including in

vivo clinical images, in order to further assess its robustness, scalability, and generalizability.

Another important direction for future work lies in the integration of the proposed framework with existing digital shade-matching systems, such as intraoral scanners and other clinically deployed imaging technologies. Such integration would facilitate the practical adoption of the approach in clinical workflows, enabling more consistent, reproducible, and perceptually grounded shade selection in everyday dental practice. More broadly, future developments will aim to strengthen the translational potential of the framework by combining broader clinical validation, adaptation to alternative shade systems, and closer integration with existing digital restorative workflows.

8. Conclusion

This work presents a perceptually grounded and extensible framework for modeling and evaluating dental shade categories through fuzzy conceptual spaces. By integrating fuzzy logic with the geometric structure of conceptual spaces, the proposed approach captures the graduality, subjectivity, and ambiguity inherent in human color perception, which are central to dental shade assessment. The implementation in the PyFCS library supports the construction of fuzzy color spaces from dental shade guides, with the 16 shades of the VITA Classical Shade Guide used as a reference example in this study.

The main contributions of this work are threefold: (i) the construction of a flexible fuzzy color space aligned with dental shade guides, (ii) the development of pixel-wise chromatic mapping and region-based analysis tools for interpretable shade visualization, and (iii) the expert-based evaluation of the resulting fuzzy representations using fuzzy similarity metrics. Together, these contributions provide an interpretable and perceptually aligned alternative to purely crisp shade-matching representations, supporting the analysis of shade ambiguity and spatial chromatic variation.

Beyond the construction of fuzzy color categories, the proposed framework enables spatially resolved chromatic mapping and expert-driven evaluation through interactive graphical modules.

The region-based evaluation experiment, conducted with twelve dental professionals under standardized visual conditions, showed the highest agreement between expert annotations and system predictions in the middle third of the tooth, which is generally considered the most relevant region for clinical shade determination. However, lower agreement and higher complete-disagreement rates were observed in the cervical and incisal regions, reflecting the greater perceptual and anatomical complexity of these areas.

Accordingly, the findings should be interpreted as preliminary evidence of expert alignment under controlled experimental conditions, rather than as definitive evidence of clinical validity or deployment readiness. The current results suggest that fuzzy conceptual spaces can provide a useful representation for capturing shade ambiguity and gradual chromatic transitions, with potential relevance for broader clinical usefulness across diverse acquisition settings, although further real-world validation, external reference measurements, and comparative testing are still required.

A further strength of the framework lies in its adaptability. Shade references can be recalibrated or substituted to align with different shade guides, acquisition settings, or institutional protocols, without modifying the core perceptual and fuzzy inference pipeline. This flexibility makes the framework suitable for further research, software development, and teaching scenarios focused on color interpretation and perceptual modeling.

Overall, the proposed framework advances dental shade analysis by combining perceptual interpretability, geometric consistency, and practical flexibility within a single open-source computational environment. Within the limits of the present controlled evaluation, it provides a promising basis for representing shade ambiguity, gradual chromatic transitions, and region-specific color variation in a form

that can support future research on shade analysis, restoration planning workflows, and clinician–technician communication. However, the framework should be regarded at this stage as an interpretability-oriented tool supported by an initial controlled evaluation, rather than as a clinically deployable shade-matching system.

CRedit authorship contribution statement

Rafael Vázquez-Conejo: Writing – original draft, Visualization, Software, Methodology, Investigation, Formal analysis, Data curation. **Maria Tejada-Casado:** Writing – review & editing, Supervision, Methodology, Investigation. **Luis Javier Herrera:** Writing – review & editing, Supervision. **Razvan Ghinea:** Writing – review & editing, Supervision, Resources. **Jose Manuel Soto-Hidalgo:** Writing – original draft, Supervision, Resources, Methodology, Investigation, Conceptualization.

Declaration of Generative AI and AI-assisted technologies in the writing process

During the preparation of this work the author(s) used GPT-4 in order to improve language and readability. After using this tool/service, the author(s) reviewed and edited the content as needed and take(s) full responsibility for the content of the publication.

Declaration of competing interest

The authors declare that they have no known competing financial interests or personal relationships that could have appeared to influence the work reported in this paper.

Acknowledgment

This research has been supported by the Project PID2022-142151OB-I00 funded by MICIU/AEI/10.13039/501100011033. Funding for open access charge: Universidad de Granada.

Data availability

Data will be made available on request.

References

- Ahmed, N., Khalid, S., Vohra, F., Halim, M.S., Al-Saleh, S., Tulbah, H.I., Al-Qahtani, A.S., Abduljabbar, T., 2024. Analysis of recurrent esthetic dental proportion of natural maxillary anterior teeth: A systematic review. *J. Prosthet. Dent.* 131 (2), 187–196.
- Alnaggar, O.A.M.F., Jagadale, B.N., Saif, M.A.N., Ghaleb, O.A.M., Ahmed, A.A.Q., Aqlan, H.A.A., Al-Arki, H.D.E., 2024. Efficient artificial intelligence approaches for medical image processing in healthcare: comprehensive review, taxonomy, and analysis. *Artif. Intell. Rev.* 57 (8), 221.
- Benavente, R., Vanrell, M., Baldrich, R., 2008. Parametric fuzzy sets for automatic color naming. *J. Opt. Soc. Am.* 25 (10), 2582–2593.
- Berlin, B., Kay, P., 1991. Basic color terms: Their universality and evolution. In: Anthropology, linguistics, psychology, University of California Press.
- Carrillo-Perez, F., Pecho, O.E., Morales, J.C., Paravina, R.D., Della Bona, A., Ghinea, R., Pulgar, R., Perez, M.D.M., Herrera, L.J., 2022. Applications of artificial intelligence in dentistry: A comprehensive review. *J. Esthet. Restor. Dent.* 34 (1), 259–280.
- Chairat, S., Chaichulee, S., Dissaneewate, T., Wangkulangkul, P., Kongpanichakul, L., 2023. AI-assisted assessment of wound tissue with automatic color and measurement calibration on images taken with a smartphone. *Healthcare* 11 (2), 273.
- Chamorro-Martínez, J., Soto-Hidalgo, J., Martínez-Jiménez, P., Sánchez, D., 2016. Fuzzy color spaces: A conceptual approach to color vision. *IEEE Trans. Fuzzy Syst.*
- Cherfi, Z., Bécharad Marinier, B.-M., Boudaoud, N., 2002. Case study: Color control in the automotive industry. *Qual. Eng.* 15, 161–170.
- Conejo, R.V., Tejada-Casado, M., Herrera, L., Guinea, R., Soto-Hidalgo, J.M., 2024. PyFCS: A new python library to create and manipulate fuzzy color spaces. In: Proceedings of the 2024 IEEE International Conference on Fuzzy Systems (FUZZ-IEEE).

- Datacolor, 2026. SpectraVision. URL <https://www.datacolor.com/es/business-solutions/product/spectravision/>, Accedido: 2026-04-09.
- Doe, J., Kumar, S., Lee, P., 2022. Bi-stage multi-modal 3D instance segmentation method for color-guided object detection. *Eng. Appl. Artif. Intell.* 130, 105412.
- Gärdenfors, P., 2000. *Conceptual Spaces - The Geometry of Thought*. The MIT Press.
- Gärdenfors, P., 2014. *The Geometry of Meaning: Semantics Based on Conceptual Spaces*. MIT Press.
- Gehrke, P., Riekeberg, U., Fackler, O., Dhom, G., 2009a. Comparison of in vivo visual, spectrophotometric and colorimetric shade determination of teeth and implant-supported crowns. *Int. J. Comput. Dent.* 12 (2), 123–132.
- Gehrke, P., Riekeberg, U., Fackler, O., Dhom, G., 2009b. Comparison of in vivo visual, spectrophotometric and colorimetric shade determination of teeth and implant-supported crowns. *Int. J. Comput. Dent.*
- Han, K., Lim, J., Ahn, J.-S., Lee, K.-S., 2025. The evaluation of a deep learning approach to automatic segmentation of teeth and shade guides for tooth shade matching using the SAM2 algorithm. *Bioengineering* 12 (9), 959.
- Hardan, L., Bourgi, R., Cuevas-Suárez, C.E., Lukomska-Szymanska, M., Monjarás-Ávila, A.J., Zarow, M., Jakubowicz, N., Jorquera, G., Ashi, T., Mancino, D., Kharouf, N., Haikel, Y., 2022. Novel Trends in Dental Color Match Using Different Shade Selection Methods: A Systematic Review and Meta-Analysis. *Materials* 15 (2), 468.
- Herrera, L.J., Pulgar, R., Santana, J., Cardona, J.C., Guillen, A., Rojas, I., Perez, M.d.M., 2010. Prediction of color change after tooth bleaching using fuzzy logic for vita classical shades identification. *Appl. Opt.* 49 (3), 422–429.
- Itten, J., 1974. *The Art of Color: the Subjective Experience and Objective Rationale of Color*. John Wiley.
- Jaffer, S.I., Al-kholani, A., 2024. A clinical comparison between new and conventional methods for quantification of intended and fabricated dental porcelain color. *Med. Clin. Sci.* 10 (1), 15–21.
- Jeong, J.-S., Kim, K.-S., Gu, Y., Yang, L.Y., Yoon, D.-H., Wang, L., Zhang, M., Kim, J.-H., 2025. Evaluation of VITA shade-based tooth color categories using deep learning. *Sci. Rep.* 15 (1), 40098.
- Jorquera, G.J., Atria, P.J., Galán, M., Feureisen, J., Imbarak, M., Kernitsky, J., Cacciuttolo, F., Hirata, R., Sampaio, C.S., 2022. A comparison of ceramic crown color difference between different shade selection methods: Visual, digital camera, and smartphone. *J. Prosthet. Dent.* 128 (4), 784–792.
- Judeh, A., Al-Wahadni, A., 2009. A comparison between conventional visual and spectrophotometric methods for shade selection. *Quintessence Int.*
- Kim, H.-S., Kim, E.J., Kim, J., 2023. The optimal color space for realistic color reproduction in virtual reality content design. *Electronics* 12 (22).
- Kim, M., Kim, B., Park, B., Lee, M., Won, Y., Kim, C.-Y., Lee, S., 2018. A digital shade-matching device for dental color determination using the support vector machine algorithm. *Sensors* 18 (9), 3051.
- Kutkut, N., Jordi, M., Almalki, A., Conejo, J., Anadioti, E., Blatz, M., 2024. Comparison of the Accuracy and Reliability of Instrumental Shade Selection Devices and Visual Shade Selection: An in Vitro Study. *J. Esthet. Restor. Dent.* 37 (2), 477–484.
- Li, Y., 2024. “Will artificial intelligence platforms replace designers in the future?” analyzing the impact of artificial intelligence platforms on the engineering design industry through color perception. *Eng. Appl. Artif. Intell.* 138, 109369.
- Li, Q., Chen, D., Wang, H., Shen, J., 2025. A machine learning based approach to standardizing tooth color and shade recommendations. *J. Prosthet. Dent.* 134 (6), 2543–2551.
- Li, L., Smith, J., García, A., Zhou, K., 2025. Learning multi-color curve for image harmonization. *Eng. Appl. Artif. Intell.* 138, 110277.
- Menegaz, G., Le Troter, A., Sequeira, J., Boí, J., 2007. A discrete model for color naming. *EURASIP J. Adv. Signal Process.* 2, 1–10.
- Morsy, N., Holiel, A.A., 2023. Color difference for shade determination with visual and instrumental methods: a systematic review and meta-analysis. *Syst. Rev.* 12 (1).
- Palmer, S.E., 1999. *Vision Science - Photons to Phenomenology*. The MIT Press.
- Parakh, A., Awate, A., Barman, S.M., Kadu, R.K., Tulaskar, D.P., Kulkarni, M.B., Bhaiyya, M., 2025. Artificial intelligence and machine learning for colorimetric detections: Techniques, applications, and future prospects. *Trends Environ. Anal. Chem.* 48, e00280.
- Paravina, R.D., Pérez, M.M., Ghinea, R., 2019. Acceptability and perceptibility thresholds in dentistry: A comprehensive review of clinical and research applications. *J. Esthet. Restor. Dent.* 31 (2), 103–112, Official publication of the American Academy of Esthetic Dentistry.
- Rashid, F., Farook, T.H., Dudley, J., 2023a. Digital shade matching in dentistry: A systematic review. *Dent. J.* 11 (1), 102–121, Meta-analysis comparing digital vs visual shade matching; highlights improved accuracy and reproducibility using digital / colorimetric devices.
- Rashid, F., Farook, T.H., Dudley, J., 2023b. Digital Shade Matching in Dentistry: A Systematic Review. *Dent. J.* 11 (11), 250.
- Rigueira, X., Martinez, J., Araujo, M., Recaman, A., 2022. Computer vision application for improved product traceability in the granite manufacturing industry.
- Rosch, E., 1975. Cognitive representations of semantic categories. *J. Exp. Psychol. [Gen.]* 104, 192–233.
- Rosch, E., 1978. Prototype classification and logical classification: The two systems. In: Scholnik, E. (Ed.), *New Trends in Cognitive Representation: Challenges To Piaget's Theory*. Lawrence Erlbaum Associates, Hillsdale, NJ, pp. 73–86.
- Ruiz-López, J., Perez, M.M., Lucena, C., Pulgar, R., López-Toruño, A., Tejada-Casado, M., Ghinea, R., 2022. Visual and instrumental coverage error of two dental shade guides: an in vivo study. *Clin. Oral Investig.* 26 (9), 5961–5968, Epub 2022 May 31.
- Şahin, N., Ural, Ç., 2024. Comparison of different digital shade selection methodologies in terms of accuracy. *J. Adv. Prosthodont.* 16 (1), 38.
- Salvi, M., Dogan, S., Inamdar, M.A., Raghavendra, U., Gudigar, A., Nitti, F., Ferraris, A., Tuncer, T., Barua, P.D., Molinari, F., Acharya, U.R., 2026. Evolution of fuzzy logic in medical applications: methods, trends and clinical applications. *Expert Syst. Appl.* 321, 132344.
- Sarpong, K., Awrangjeb, M., Islam, M.S., 2025. Dual spectral-spatial residual adaptive network for hyperspectral image classification in the presence of noisy labels. *Eng. Appl. Artif. Intell.* 142, 109900.
- Shetty, S., Gali, S., Augustine, D., Sv, S., 2024. Artificial intelligence systems in dental shade-matching: A systematic review. *J. Prosthodont.* 33 (6), 519–532.
- Smeulders, A., Worring, M., Santini, S., Gupta, A., Jain, R., 2000. Content-based image retrieval at the end of the early years. *IEEE Trans. Pattern Anal. Mach. Intell.* 22 (12), 1349–1380.
- Song, S., Jia, Z., Shi, F., Wang, J., Ni, D., 2024. Adaptive fuzzy weighted C-mean image segmentation algorithm combining a new distance metric and prior entropy. *Eng. Appl. Artif. Intell.* 131, 107776.
- Soto-Hidalgo, J., Martínez-Jiménez, P., Chamorro-Martínez, J., Sánchez, D., 2016. JFCS: A color modeling java software based on fuzzy color spaces. *IEEE Comput. Intell. Mag.* 11 (2), 16–28.
- Tabatabaian, F., Beyabanaki, E., Alirezaei, P., Epakchi, S., 2021. Visual and digital tooth shade selection methods, related effective factors and conditions, and their accuracy and precision: A literature review. *J. Esthet. Restor. Dent.* 33 (8), 1084–1104.
- Tam, W.-K., Lee, H.-J., 2017. Accurate shade image matching by using a smartphone camera. *J. Prosthodont. Res.* 61 (2), 168–176.
- Tejada-Casado, M., Pérez, M.M., Della Bona, A., Lübbe, H., Ghinea, R., Herrera, L.J., 2024. Chroma-dependence of CIEDE2000 acceptability thresholds for dentistry. *J. Esthet. Restor. Dent.* 36 (3), 469–476, Epub 2023 Oct 20.
- Vázquez-Conejo, R., Tejada-Casado, M., Herrera, L.J., Ghinea, R., Soto-Hidalgo, J.M., 2025. PyFCS GUI: A new visualization and interaction framework for fuzzy color spaces. *SoftwareX* 31, 102316.
- VITA Zahnfabrik, 2025. VITA classical A1-d4® shade guide – the original for the PERFECT MATCH in your choice of color. (Accessed 24 March 2025).
- Wang, Z., Dong, Y., Sui, X., Shao, X., Li, K., Zhang, H., Xu, Z., Zhang, D., 2024. An artificial intelligence-assisted microfluidic colorimetric wearable sensor system for monitoring of key tear biomarkers. *Npj Flex. Electron.* 8 (1), 35.
- Wei, T., Wang, X., Li, X., Zhu, S., 2022. Fuzzy subspace clustering noisy image segmentation algorithm with adaptive local variance & non-local information and mean membership linking. *Eng. Appl. Artif. Intell.* 110, 104672.
- Xu, J., Li, K., Li, Z., Chong, Q., Xing, H., Xing, Q., Ni, M., 2024. Fuzzy graph convolutional network for hyperspectral image classification. *Eng. Appl. Artif. Intell.* 127, 107280.